

Cohesive Properties of Cu-X and Ni-X (In, Sn) Intermetallics: Ab Initio Systematics, Correlations and “Universality” Features

Dalía S. Bertoldi¹ · S. B. Ramos^{1,2} · N. V. González Lemus¹ · A. Fernández Guillermet^{2,3}

Submitted: 15 November 2016 / in revised form: 20 February 2017
© ASM International 2017

Abstract This paper reports an analysis of the systematics of cohesive properties and equation-of-state parameters for a large number of stable, metastable and hypothetical binary Me_aX_b type phases formed by $\text{Me} = \text{Cu}, \text{Ni}$ with $\text{X} = \text{In}, \text{Sn}$. To this aim, an ab initio database previously developed by the authors using spin polarized density-functional-theory calculations, using the VASP code, is adopted. The work involves the volume (V_0), Wigner–Seitz radius, bulk modulus (B_0) and cohesive energy (E_{coh}) of the phases. At the outset of the paper it is shown that these properties can be studied as functions of the average group number (AGN), i.e., the weighted average of the number of valence electrons involved in the VASP calculations. Moreover, the cohesive energy density (CED), defined as E_{coh}/V_0 , is shown to correlate very well with the AGN variable and with B_0 . These striking regularities are given two complementary interpretations. First, a general microscopic picture of the variations of cohesion is developed by studying the evolution of the contributions of the d - and p -electrons to their electronic density of states.

In this way the effects of the hybridization of d - and p -electrons, and the filling up of bonding and anti-bonding states is highlighted. Next, a thermodynamic analysis based on the classical approach developed by Rose, Ferrante, Smith and collaborators is performed. It is concluded that the correlation involving CED and B_0 is a manifestation of a significant degree of “universality” in the variation of the cohesive properties with the Wigner–Seitz radius of these compounds.

Keywords ab initio · cohesive properties · intermetallics · lead-free soldering alloys

1 Introduction

Ab initio calculations are currently recognized as a powerful route to the theoretical account of the phase-stability properties of elements and compounds. In particular, by using these methods it is possible to develop rather comprehensive databases with various types of quantities of interest in the thermodynamic calculation of phase diagrams using the phenomenological *CALPHAD* techniques. From a more fundamental point of view, ab initio techniques offer the possibility to search for the ground state structures in an alloy system, and access to the cohesive and equation-of-state (EOS) parameters for stable, non-stable and even hypothetical phases of the type involved in, e.g., the application of the thermodynamic compound energy formalism.^[1]

When such studies are performed for a given class of compounds, the approach might also lead to interrelations between various types of properties, which in turn could be interpreted in microscopic terms by using the ab initio information on the electronic structure. The detailed and

This article is an invited paper selected from presentations at TOFA 2016, the Discussion Meeting on Thermodynamics of Alloys, held September 4-9, 2016, in Santos, Brazil, and has been expanded from the original presentation.

✉ A. Fernández Guillermet
a.f.guillermet@gmail.com

- ¹ Instituto de Investigación y Desarrollo en Ingeniería de Procesos, Biotecnología y Energías Alternativas, CONICET - UNCo, Neuquén, Argentina
- ² Departamento de Física, Facultad de Ingeniería, Universidad Nacional del Comahue, Neuquén, Argentina
- ³ CONICET - Centro Atómico Bariloche e Instituto Balseiro, Neuquén, Argentina

reliable picture of the systematics of cohesive properties established in this way might be useful as a complement of the experimental database and a valuable tool in the assessment and estimation of lacking information.

The general purpose of the present paper is to test these attractive possibilities by using a recently developed ab initio database with information on a specific family of compounds, viz., the binary Me_aX_b type phases formed by $\text{Me} = \text{Cu}, \text{Ni}$ with $\text{X} = \text{In}, \text{Sn}$. A practical motivation of the work is the need to design new alloys for lead-free soldering applications.^[2] Since the In–Sn alloy has long been recognized as a promising candidate for Cu and Ni contact materials,^[3] there has been long-standing interest in characterizing the stability and properties of the key structures formed upon soldering, viz., the intermetallic compounds (ICs) occurring in the Cu–In–Sn^[4–7] and Ni–In–Sn alloys.^[8,9]

In particular, the current authors have previously determined ab initio the thermodynamic properties and electronic structure of a large group of stable, metastable and hypothetical ICs in the Cu–In and Cu–Sn,^[10] Ni–In and Ni–Sn^[11,12] binary subsystems. As a first application of the ab initio database developed in this way, the systematic effects of replacing Cu by Ni in several stable and non-stable Me_aX_b ICs were established.^[13] The general aim of the present study is to extend this line of research and use the theoretical database to establish the systematics and interrelations between cohesive properties and EOS parameters for this class of compounds. In the following we present the specific purposes of the study.

The first purpose is to test the use of the average number of electrons per atom (expressed as the “average group number”, *AGN*) in the Me_aX_b compounds as a useful coordinate to systematize and reveal similarities in the trends in cohesive properties of the Cu–X and Ni–X ($\text{X} = \text{In}, \text{Sn}$) phases. This possibility is hinted at by early studies of the *p*–*d* bonded structures suggesting that various cohesion-related properties of compounds formed by transition metals with non-metals could be expressed as smoothly varying functions of the *AGN* variable.^[14–20] In the current study the applicability of these previous findings to establish trends in the variation of V_0 , B_0 and E_{coh} of Me_aX_b type phases ($\text{Me} = \text{Cu}, \text{Ni}$ and $\text{X} = \text{In}, \text{Sn}$) will be tested using results of density-functional-theory (DFT) ab initio calculations performed by means of the projected augmented waves (PAW) method, as implemented in the “Vienna Ab initio Simulation Package” (VASP) code.

The second purpose is to explore the possibility of establishing rather general interrelations between two cohesion-related properties with dimensions of pressure, viz., the bulk modulus (B_0) and the ratio (E_{coh}/V_0). This part of the study was stimulated by classical^[21] and more recent^[22] empirical attempts to correlate these quantities

using experimental data on the elemental solids. In the present study these previous ideas will be tested by using the ab initio results for a large group of ICs. In addition, a phenomenological interpretation of the relation between B_0 and E_{coh}/V_0 will be developed by using the approach applied long ago to elements by Rose, Ferrante and Smith and collaborators, which was based on hypothesizing the existence of a universal binding energy relation.^[23,24]

The third purpose of the paper is to develop a microscopic picture of the trends in cohesion of the *p*–*d* bonded compounds, on the basis of the pioneering work by Gelatt et al.^[25] as well as other classical theoretical^[26–30] and experimental^[31] studies of the electronic structure of the transition metals and their compounds.

2 Theoretical Method and Ab Initio Database

The present work is based on ab initio results obtained from spin polarized total energy DFT calculations, performed using the PAW method^[32,33] and the VASP code.^[34] The technical details of how the calculations were performed are described in Ref 10 and 11. Here we just mention a few aspects of relevance for the present study. We used the exchange-correlation energy in the generalized gradient approximation by Perdew and Wang (GGA-PW91).^[35] The number of valence electrons considered was 11 for Cu ($3d^{10}4s^1$), 10 for Ni ($3d^84s^2$), 3 for In ($5s^2p^1$) and 4 for Sn ($5s^2p^2$).

With the given numbers of valence electrons of the Me elements (n_{Me}) and X elements (n_{X}), the *AGN* parameter for the compound Me_aX_b was calculated as

$$AGN = (a + b)^{-1}(an_{\text{Me}} + bn_{\text{X}}) \quad (\text{Eq 1})$$

The cut-off kinetic energy for the expansion of plane waves was 314 eV for the Cu–X compounds and 330 eV for Ni–X compounds ($\text{X} = \text{In}, \text{Sn}$). These values were tested to guarantee convergence in total and cohesive energies, within 10 and 2 meV/atom, respectively.

The Monkhorst–Pack k-point meshes^[36] were used to map the Brillouin zone chosen to converge within 1 meV/atom, and the Methfessel–Paxton technique^[37] for the occupation of the electronic levels (smearing factor of 0.1). The criterion for the self-consistent convergence of the total energy was 0.1 meV, the energy variations due to changes in the structural degrees of freedom were lower than 1 meV/atom, with forces on the ions lower than 30 meV/Å.

The cohesive energy (E_{coh}) per atom of the Me_aX_b compound was obtained, as described in Ref 12, by computing the difference between the total energy per atom of the compound at the equilibrium volume (V_0) and the weighted average atomic energy (“at”) of the isolated

Me = Cu, Ni (“ E_{Me} ”) and X = Sn, In (“ E_X ”) atoms in their corresponding ground state electronic configuration, as follows:

$$E_{\text{coh}} = \left(\frac{1}{a+b} \right) (aE_{\text{Me}}^{\text{at}} + bE_X^{\text{at}} - E^{\text{tot}}(V_0)) \quad (\text{Eq 2})$$

The energy of the free atoms was calculated by placing an isolated atom in a sufficiently large cubic supercell. Specifically, a lattice parameter of up to 20 Å was adopted. The Brillouin zone was mapped only at the Γ point, and for the occupation of the electronic levels a small smearing factor (0.001 eV) was used, as recommended. Since the experimental atomic ground states might be different from the configurations for which the potential was generated,

Table 1 The number of valence electrons per atom of the Me (=Cu, Ni) elements (n_{Me}) and X (=In, Sn) elements (n_X) and the calculated cohesive energy, equilibrium atomic volume and bulk modulus for the elements Cu, Ni, In and Sn

Phase	n_{Me}, n_X	V_0	r_0	E_{coh}	B_0	λ
Ni (cF4)	10	10.931	1.377	495.126	186.2	0.212
Cu (fcc)	11	12.027	1.421	338.938	142.3	0.191
In (tI2)	3	27.505	1.872	233.096	36.5	0.207
Sn (tI4)	4	28.348	1.891	309.382	48.6	0.203

The equilibrium volume (V_0) is given in Å³/atom, the Wigner–Seitz radius [$r_0 = (3/4\pi V_0)^{1/3}$] in Å, the cohesive energy (E_{coh}) in kJ/mol, the bulk modulus (B_0) in GPa, and the λ parameter in dimensionless units

Table 2 The average group number (AGN) and the calculated cohesive energy, equilibrium atomic volume and bulk modulus for stable, metastable, ideal and hypothetical Cu–In intermetallic phases

Phase	AGN	V_0	r_0	E_{coh}	B_0	λ
Stable						
Cu ₇ In ₃ (aP40)	8.6	15.096	1.533	308.620	99.3	0.195
Cu ₉ In ₄ (cP52)	8.5	15.143	1.534	306.353	101.1	0.192
Cu ₁₀ In ₇ (mC68)	7.7	16.841	1.590	297.280	86.2	0.194
Cu ₁₁ In ₉ (mC20)	7.4	17.369	1.606	292.330	81.5	0.195
CuIn ₂ (tI12)	5.7	20.506	1.698	268.738	62.6	0.197
Ideal						
Cu ₂ In (hP6)	8.3	15.534	1.548	296.265	92.1	0.195
CuIn (hP4)	7.0	19.415	1.667	283.772	76.3	0.188
CuIn ₂ (hP6)	5.7	22.131	1.742	253.332	49.9	0.205
Hypothetical						
Cu ₄ In (cF16)	9.4			308.916		
Cu ₃ In (oP8)	9.2	14.488	1.512	311.949		
Cu ₅ In ₄ - η_1 (mP36)	7.4	17.873	1.622	293.170		
Cu ₅ In ₄ - η_2 (mC54)	7.4	17.889	1.622	293.017		
Cu ₆ In ₅ - η (mC44)	7.4	18.144	1.628	291.800		
Cu ₃ In (hP8)	9.2	14.628	1.517	331.919	106.78	0.198

The equilibrium volume (V_0) is given in Å³/atom, the Wigner–Seitz radius [$r_0 = (3/4\pi V_0)^{1/3}$] in Å, the cohesive energy (E_{coh}) in kJ/mol, the bulk modulus (B_0) in GPa, and the λ parameter in dimensionless units

the correct occupation numbers were taken by fixing the difference between spins up and down along the run.

3 Systematics of Cohesive Properties

In Tables 1, 2, 3, 4 and 5 we summarize the structural and cohesive properties of the ICs analyzed in the present work. There we list the $T = 0$ K values of the volume per atom (V_0), Wigner–Seitz radius r_0 [defined as $r_0 = (3/4\pi V_0)^{1/3}$], bulk modulus (B_0) and cohesive energy (E_{coh}). The calculated properties of the elements Cu, Ni, In and Sn are presented in Table 1, and those of the stable, metastable and hypothetical Cu–In and Cu–Sn,^[10] Ni–In and Ni–Sn^[11,12] systems, 56 in total, summarized in Ref 13, are listed in Tables 2, 3, 4 and 5. The lattice parameters, from which we get V_0 for the currently treated elements and compounds, were presented and compared elsewhere^[10,11] with the available experimental data and previously reported ab initio calculations.

In those previous works,^[10,11] comparisons with data for B_0 for the elements were also presented, but it was remarked that the information on the elastic properties of the ICs is scarce. In view of this fact, in Tables 2, 3, 4 and 5 we added experimental values for B_0 at room temperature measured by Ghosh^[38] and Mikhaylushkin et al.^[39] With the exception of the NiIn (hP6) compound, there is good agreement between their experimental values and the current ab initio results.

3.1 Cohesive Properties Versus Average Group Number Plots

The calculated values (symbols) of V_0 , r_0 , B_0 and E_{coh} , of the Cu-X ($X = \text{In, Sn}$) ICs are plotted versus the AGN of the compounds in Fig. 1(a), (c), (e), and (g), respectively. The corresponding values of the Ni-X ($X = \text{In, Sn}$) are plotted using symbols in Fig. 1(b), (d), (f), and (h) respectively. The dotted lines in these plots are only guides to the eye. The symbols labeled “stable” refer to the ground state structures. These graphics indicate that V_0 (and r_0) for the Cu-X as well as the Ni-X compounds decreases, whereas B_0 and E_{coh} , increases with the increase in the AGN . The variations with AGN are fairly smooth for Cu-X and the Ni-X ICs. The only points deviating from the scatter band trend correspond to the hypothetical compounds “NiIn” (hP4) and “NiSn” (hP4).

A further analysis of the dependence upon AGN will be performed by focusing on the ratio E_{coh}/V_0 which will be referred to in the following as “cohesive energy density”

(CED). The CED versus AGN values for Cu-X ($X = \text{In, Sn}$) and Ni-X ($X = \text{In, Sn}$) are plotted using symbols in Fig. 2(a) and (b) respectively. The dotted lines are only guides to the eye. The symbols labeled “stable” refer to the ground state structures. In spite of the various structures involved, the CED values for Cu-X (Fig. 2a) compounds determine a single (dotted) line, and so do most of the values for Ni-X compounds (Fig. 2b). As before, the only points in Fig. 2 deviating from the well-defined lines correspond to the hypothetical compounds “NiIn” (hP4) and “NiSn” (hP4).

In view of the existence of the correlations shown by the CED versus AGN plots, it is natural to move one step forward and explore the existence of interrelations between the key cohesive properties of this family of ICs.

3.2 Bulk Modulus Versus Cohesive Energy Density Plots

Recent empirical^[22] and theoretical^[40] studies of the thermophysical properties of the elements suggest that B_0

Table 3 The average group number (AGN) and the calculated cohesive energy, equilibrium atomic volume and bulk modulus for stable, metastable, ideal and hypothetical Cu–Sn intermetallic phases

Phase	AGN	V_0	r_0	E_{coh}	B_0	λ
Stable						
Cu ₄ Sn (cF16)	9.6	14.726	1.520	326.030	99.6	0.203
Cu ₁₀ Sn ₃ (hP26)	9.4	14.506	1.513	331.739	109.4	0.196
Cu ₃ Sn (oP8)	9.2	14.701	1.519	331.900	104.2	0.200
Cu ₃ Sn (oP80)	9.2	14.683	1.519	331.750	101.8	0.202
Cu ₅ Sn ₄ - η_1 (mP36)	7.9	18.220	1.632	328.971	113.8(a) 81.7	0.202
Cu ₅ Sn ₄ - η_2 (mC54)	7.9	18.239	1.633	328.620	81.1 84.6(a)	0.203
Cu ₆ Sn ₅ - η (mC44)	7.8	18.428	1.638	329.057	80.9 84.4(a)	0.202
Ideal						
Cu ₂ Sn (hP6)	8.7	16.366	1.575	315.368	87.9	0.201
CuSn (hP4)	7.5	19.335	1.665	329.061	75.1	0.204
CuSn ₂ (hP6)	6.3	23.413	1.775	304.334	50.2	0.219
Hypothetical						
Cu ₇ Sn ₃ (aP40)	8.9	15.622	1.551	327.904		
Cu ₁₀ Sn ₇ (mC68)	8.1	17.628	1.614	323.132		
Cu ₁₁ Sn ₉ (mC20)	7.8	18.39	1.637	320.551		
CuSn ₂ (tI12)	6.3	21.566	1.724	317.460		

The equilibrium volume (V_0) is given in $\text{\AA}^3/\text{atom}$, the Wigner–Seitz radius [$r_0 = (3/4\pi V_0)^{1/3}$] in \AA , the cohesive energy (E_{coh}) in kJ/mol, the bulk modulus (B_0) in GPa, and the λ parameter in dimensionless units. Experimental values of B_0 from Ref 38 are included. (a) Experimental value^[38]

Table 4 The average group number (*AGN*) and the calculated cohesive energy, equilibrium atomic volume and bulk modulus for stable, metastable, ideal and hypothetical Ni–In intermetallic phases

Phase	<i>AGN</i>	V_0	r_0	E_{coh}	B_0	λ
Stable						
Ni ₃ In (hP8)	8.2	13.192	1.466	437.589	149.6	0.202
Ni ₃ In (cP4)	8.2	13.152	1.464	435.339	151.1	0.201
Ni ₇ In ₃ (aP40)	7.9	13.826	1.489	426.723	138.3	0.203
Ni ₂ In (hP6)	7.7	14.158	1.501	412.307	143.6	0.193
Ni ₅ In ₃ (mC32)	7.4	14.793	1.523	409.859	124.3	0.203
Ni ₁₃ In ₉ (mC44)	7.1	15.078	1.532	401.256	131.4	0.193
NiIn (hP6)	6.5	17.635	1.615	384.792	99.5	0.201
					153(a)	
Ni ₂ In ₃ (hP5)	5.8	18.278	1.634	355.758	94.5	0.195
Ni ₃ In ₇ (cI40)	5.1	20.090	1.687	326.732	77.1	0.197
Hypothetical						
Ni ₃ In ₂ (oP20)	7.2	15.482	1.546	404.890		
NiIn (hP4)	6.5	17.942	1.624	371.338	95.2	0.200
NiIn (hP4)	6.5	21.734	1.731	336.034	64.3	0.211
Ni ₃ In ₄ (mC14)	6.0	18.553	1.642	358.192		
NiIn ₄ (oC20)	4.4	23.392	1.774	290.855		

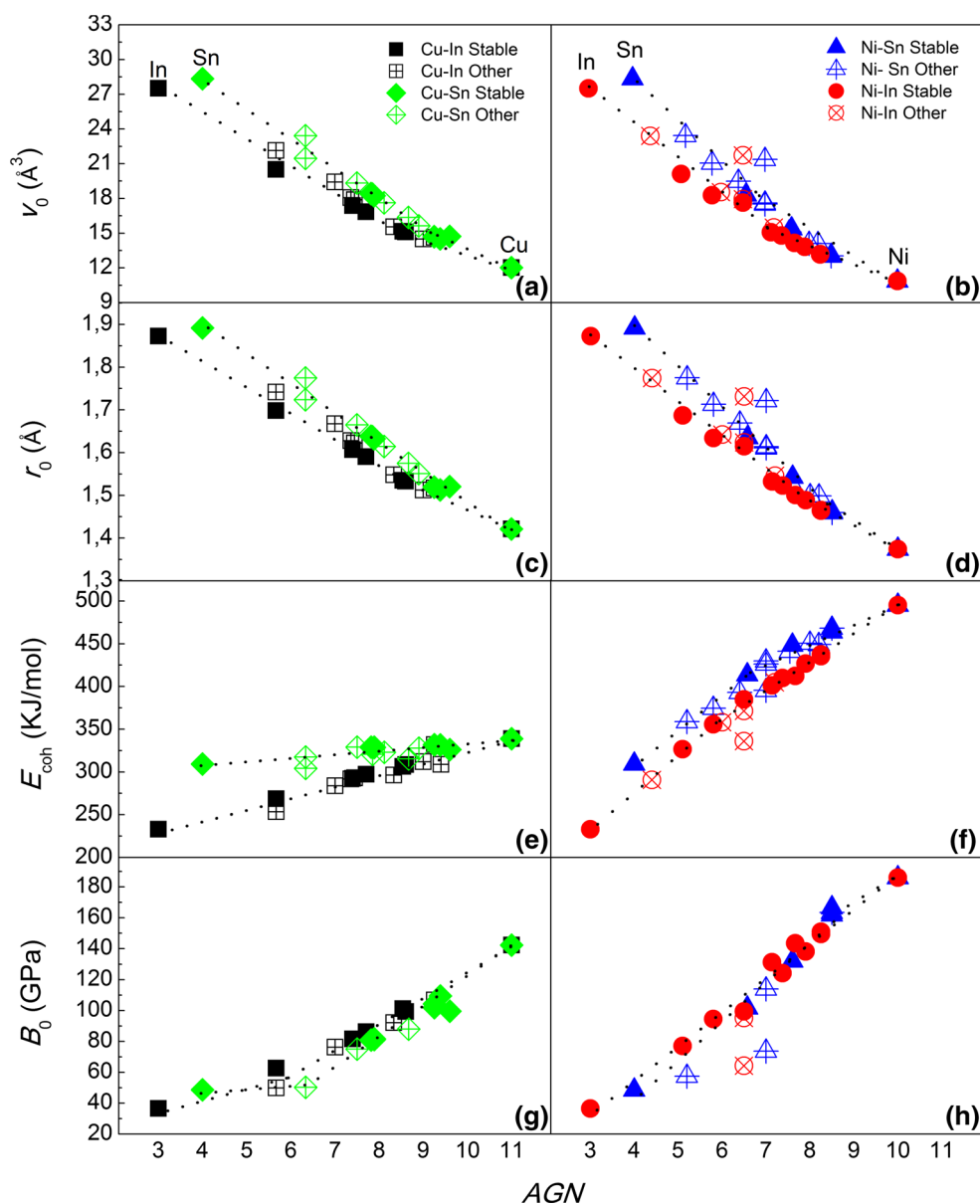
The equilibrium volume (V_0) is given in Å³/atom, the Wigner–Seitz radius [$r_0 = (3/4\pi V_0)^{1/3}$] in Å, the cohesive energy (E_{coh}) in kJ/mol, the bulk modulus (B_0) in GPa, and the λ parameter in dimensionless units. An experimental value of B_0 from Ref 39 is included. (a) Experimental value^[39]

Table 5 The average group number (*AGN*) and the calculated cohesive energy, equilibrium atomic volume and bulk modulus for stable, metastable, ideal and hypothetical Ni–Sn intermetallic phases

Phase	<i>AGN</i>	V_0	r_0	E_{coh}	B_0	λ
Stable						
Ni ₃ Sn (hP8)	8.5	13.021	1.459	468.121	166.7	0.199
Ni ₃ Sn (cF16)	8.5	13.086	1.462	463.817	162.0	0.201
Ni ₃ Sn ₂ (oP20)	7.6	15.381	1.543	448.457	132.1	0.201
Ni ₃ Sn ₄ (mC14)	6.6	18.304	1.635	413.737	101.8	0.202
					108.4(a)	
Metastable						
Ni ₃ Sn (cP4)	8.5	13.030	1.46	468.173	163.6	0.201
NiSn ₄ (oC20)	5.2	23.433	1.775	358.961	57.5	0.221
Hypothetical						
Ni ₂ Sn (hP6)	8.0	14.115	1.499	450.606		
Ni ₇ Sn ₃ (aP40)	8.2	14.117	1.499	449.107		
Ni ₁₃ Sn ₉ (mC44)	7.5	15.090	1.533	441.295		
NiSn (hp6)	7.0	17.612	1.614	426.385		
NiSn (hP4)	7.0	17.514	1.611	429.943		
NiSn (hP4)	7.0	21.374	1.722	395.500		
Ni ₂ Sn ₃ (hP5)	6.4	19.486	1.669	392.962		
Ni ₃ Sn ₇ (cI40)	5.8	21.057	1.713	374.571		

The equilibrium volume (V_0) is given in Å³/atom, the Wigner–Seitz radius [$r_0 = (3/4\pi V_0)^{1/3}$] in Å, the cohesive energy (E_{coh}) in kJ/mol, the bulk modulus (B_0) in GPa, and the λ parameter in dimensionless units. An experimental value of B_0 from Ref 38 is included. (a) Experimental value^[38]

Fig. 1 Ab initio values of the volume per atom (V_0), Wigner–Seitz radius (r_0), cohesive energy (E_{coh}) and bulk modulus (B_0) (various symbols), vs. the average group number (AGN) of Cu-X and Ni-X compounds ($X = \text{In, Sn}$). The symbols labeled “stable” refer to the ground state structures and “other” refer to ideal, metastable and hypothetical structures. The AGN parameter is defined in section 2. The dotted lines are only guides to the eye



and the CED parameter might be proportional. Such possibility is tested in Fig. 3 by plotting versus E_{coh}/V_0 the B_0 values obtained ab initio for the Cu-X (Fig. 3a) and Ni-X (Fig. 3b) compounds. It is evident that the B_0 versus E_{coh}/V_0 interrelation for the Cu-X and the Ni-X compounds can be described by a proportionality. The specific relations established by performing least-squares fits to these results are indicated by the dashed lines. The points representing In and Sn are well accounted for by the dashed lines, whereas small deviations are observed for Cu (Fig. 3a) and Ni (Fig. 3b) suggesting that for these elements the proportionality constant of the B_0 versus E_{coh}/V_0 relation should be larger (smaller) than for the Cu-X (Ni-X) compounds. In the following section, a thermodynamic

approach will be applied to develop an interpretation of the B_0 versus E_{coh}/V_0 relation.

4 Thermodynamic Analysis of “Universality” Features

4.1 Definitions and Thermodynamic Relations

Following the pioneering work by Rose et al.,^[23,24] early ab initio studies^[41] and very recent treatments^[40] of the cohesive properties of transition metals, the volume dependence of the 0 K total energy per atom [$E^{\text{tot}}(V)$] of the compound Me_aX_b with a volume V , referred to the

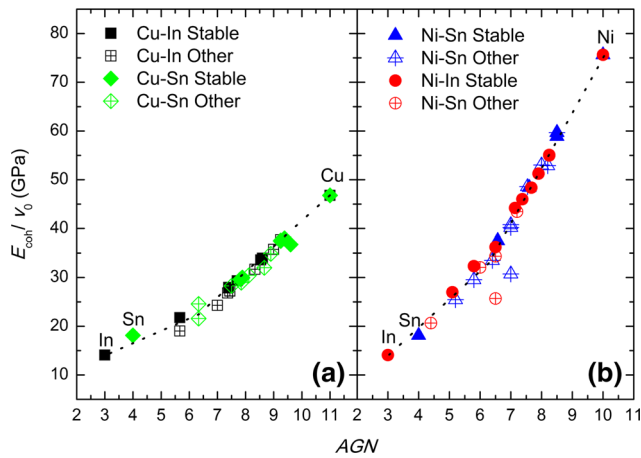


Fig. 2 Ab initio values of the cohesive energy density parameter (E_{coh}/V_0) for Cu-X (a) and Ni-X (b) compounds ($X = \text{In, Sn}$) (various symbols) vs. the average group number (AGN) parameter. The symbols labeled “stable” refer to the ground state structures and “other” refer to ideal, metastable and hypothetical structures. The dotted lines are only guides to the eye

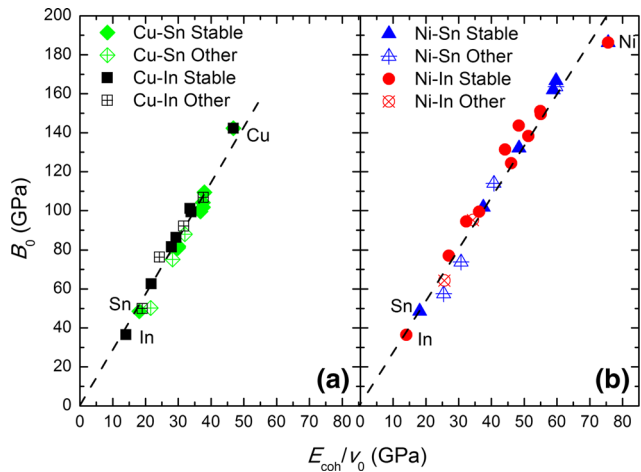


Fig. 3 Ab initio values of the bulk modulus (B_0) of Cu-X (a) and Ni-X (b) compounds ($X = \text{In, Sn}$) (various symbols) vs. the cohesive energy density parameter (E_{coh}/V_0). The symbols labeled “stable” refer to the ground state structures and “other” refer to ideal, metastable and hypothetical structures. The dashed lines represent least-squares fits

weighted average of that of the free atoms of the element “j” (E_j^{at}) ($j = \text{Cu, Ni, In, Sn}$), viz., the quantity $\left(\frac{1}{a+b}\right)(E^{\text{tot}}(V) - aE_{\text{Me}}^{\text{at}} - bE_{\text{X}}^{\text{at}})$ will be described as follows:

$$\left(\frac{1}{a+b}\right)[E^{\text{tot}}(V) - (aE_{\text{Me}}^{\text{at}} + bE_{\text{X}}^{\text{at}})] = E_{\text{coh}}F(z) \quad (\text{Eq 3})$$

where E_{coh} is given in Eq 2, and $F(z)$ is a dimensionless function of the variable z defined as:

$$z = \frac{r - r_0}{l} \quad (\text{Eq 4})$$

In Eq 4 $r = (3/4\pi V)^{1/3}$ is the Wigner-Seitz radius corresponding to the volume V , and l is material-dependent scaling length. For each compound, such scaling length can be evaluated from the E^{tot} versus V relation obtained ab initio by the following relation,

$$B_0 = \left(\frac{1}{3}\lambda\right)^2 \left(\frac{E_{\text{coh}}}{V_0}\right) \quad (\text{Eq 5})$$

where the parameter λ is defined as

$$\lambda = \frac{l}{r_0} \quad (\text{Eq 6})$$

Equation 5, early derived in Ref 40 by applying thermodynamic relations to Eq 3, and assuming for the F function and its first (F') and second (F'') derivatives with respect to z (evaluated at $z = 0$) the “universal” values $F(0) = -1$, $F'(0) = 0$ and $F''(0) = 1$ has recently been tested using an extensive ab initio and experimental database for the transition elements.^[41] In the following the applicability of this formalism to the cohesive properties of the present class of ICs will also be tested.

4.2 Systematics and “Universality” Features

The individual λ parameters for the Me_aX_b compounds ($\text{Me} = \text{Cu, Ni}$, $\text{X} = \text{In, Sn}$) obtained by applying Eq 5 and 6 to the current ab initio values are listed in Tables 1, 2, 3, 4 and 5. By using these parameters and the respective E^{tot} versus V obtained ab initio, the $F(z)$ versus z relation for each compound were established. The results, for various groups of Cu-X and Ni-X compounds are shown in Fig. 4. It is evident that a single $F(z)$ versus z relation is applicable to the Cu-X compounds (Fig. 4a, b), and a similar result is found for the Ni-X compounds (Fig. 4c, d). The possibility of establishing these $F(z)$ versus z relations is considered as indications that a “first degree of universality” exists in the cohesive behavior of the Cu-X compounds and in the Ni-X compounds.

A further, even “higher degree of universality” is found by analyzing the individual λ parameters of Cu-X (Tables 2, 3) and Ni-X (Tables 4, 5) compounds. For both families of compounds the λ values fall in essentially the same, relatively narrow range, viz., $0.19 < \lambda < 0.22$. This implies, in the first place, that for each class of compounds, the proportionality constants between B_0 and E_{coh}/V_0 viz., $(1/3\lambda)^2$ according to Eq 5, would be very close, and the respective plots of the B_0 versus E_{coh}/V_0 , values would yield approximate linear relations. This expectation is nicely corroborated for Cu-X and Ni-X compounds in Fig. 3(a) and (b), respectively.

In the second place, we note that the dashed lines obtained by least-squares fits correspond to the average

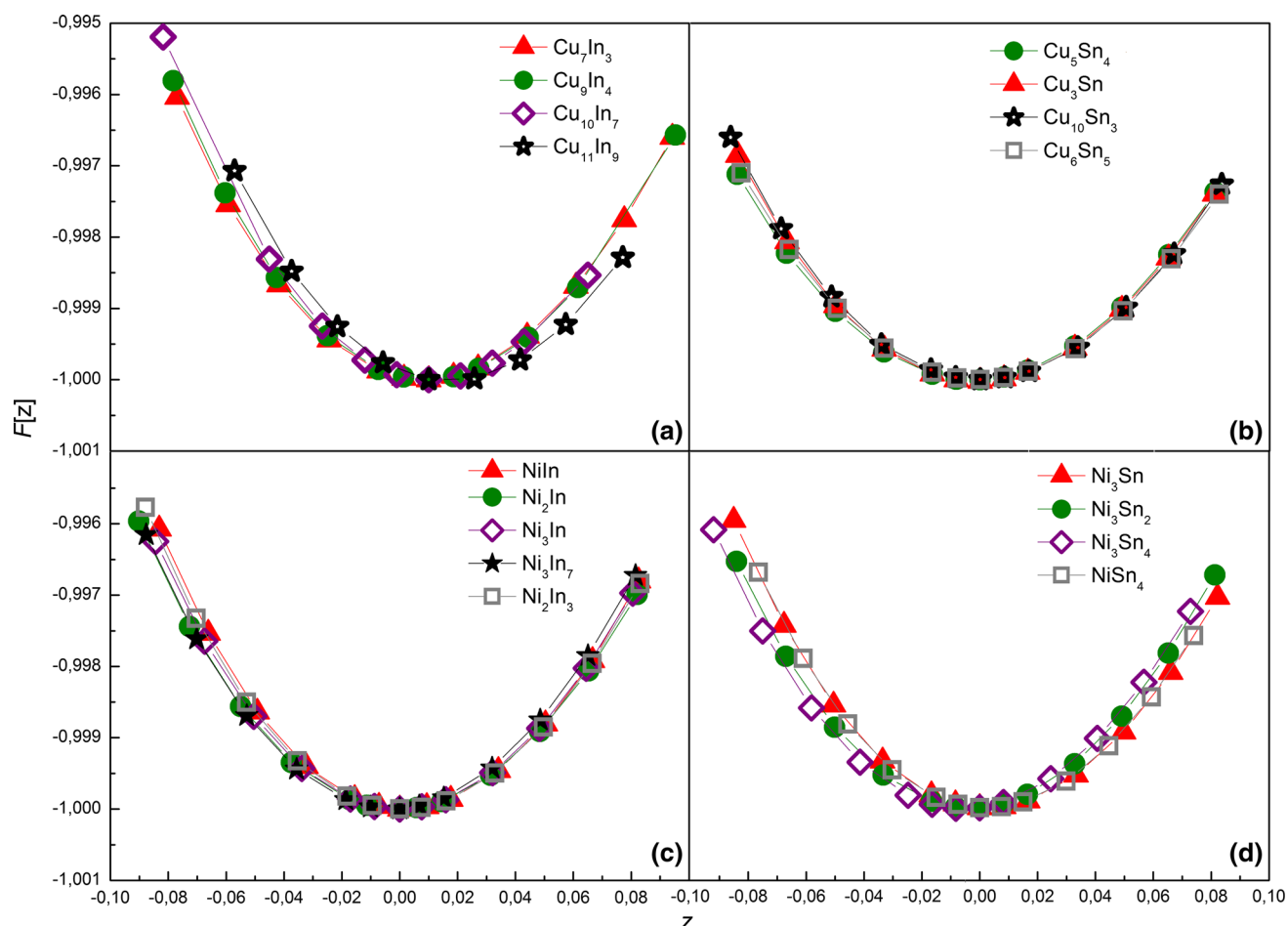


Fig. 4 Ab initio values of the $F(z)$ vs. z relation defined in section 4 for Cu-In (a), Cu-Sn (b), Ni-In (c) and Ni-Sn (d) compounds ($X = \text{In, Sn}$) (various symbols). The thin solid lines are only guides to the eye

values $0.199 (\pm 0.001)$ and $0.204 (\pm 0.002)$ of the parameter λ , respectively. Indeed, the fact that these averages are almost identical indicates that what we have called “higher degree of universality” holds for the whole family of Me_aX_b ($\text{Me} = \text{Cu, Ni}$ and $\text{X} = \text{In, Sn}$) compounds considered in the present work.

5 Systematic Aspects of the Electronic Structure of p - d Bonded Compounds

Encouraged by the systematics of cohesive properties and the interrelations between cohesive and EOS parameters for the (Cu, Ni)(In, Sn) ICs, in this section we study the electronic properties of this family of compounds, in order to provide a general microscopic picture of the trends in binding forces in terms of the electronic structure. To this end we will select various binary IPs formed by combining Ni or Cu and In or Sn, and compare the evolution of the various contributions to the electronic density-of-states (DOS) and the chemical bonding, as a function of the

elements constituting the compounds and their stoichiometry.

One important observation concerning the previously discussed correlations as a function of the AGN , is the fact that they involve a large number of compounds despite their very different structures. As stated previously, these correlations and trends are found to be almost insensitive to the specific structure of the compounds. The DOS of a compound is known to be strongly structure dependent. However, E_{coh} as expressed in simple electron band models can be related to the integrated DOS, therefore being less sensitive to details of the band structure. In fact, empirical electron band models employing a rectangular d -band electron DOS, only including band structure parameters like bandwidth and relative positions of the bands, could explain satisfactorily the main features of cohesion and the energetic of transition metal alloys formation.^[26-29]

For the type of compounds investigated here, the most important features of their electronic structure have been described in a previous work^[13] by considering the DOS of various representative iso-structural Me-X compounds

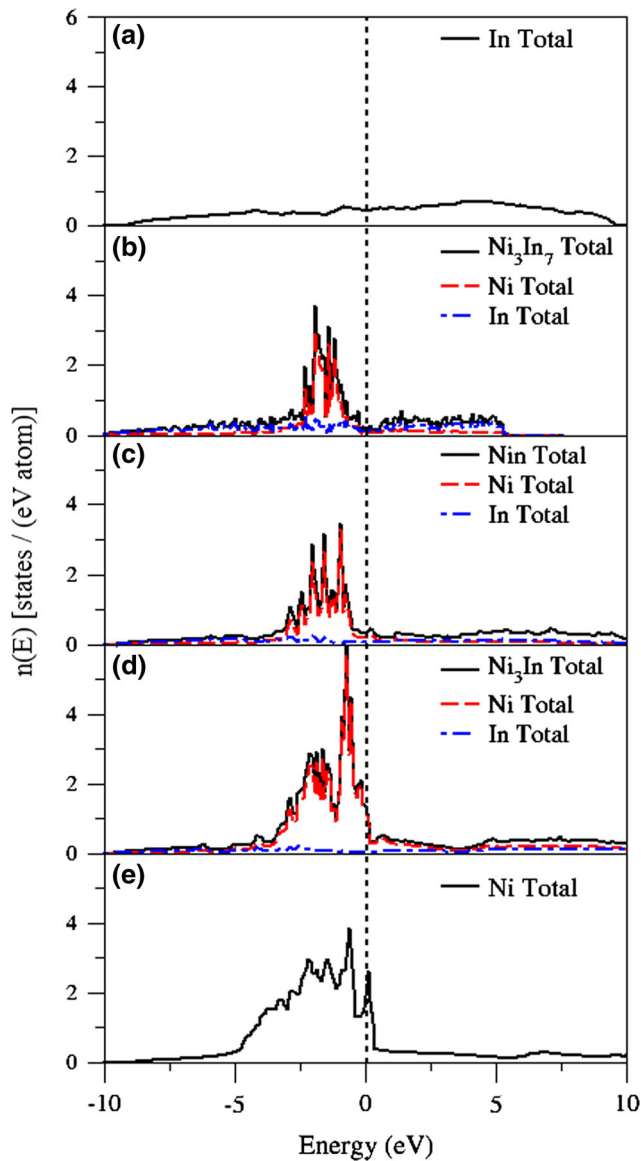


Fig. 5 Electronic density of states (DOS) for (a) In (tI2), (b) Ni_3In_7 (cI40), (c) NiIn (hP6), (d) Ni_3In (hP8), and (e) Ni (cF4). The atomic decomposed In (blue dash-dot lines) and Ni (red dashed lines) partial DOS are shown. The origin of the scale corresponds to the Fermi level (Color figure online)

(Me = Cu, Ni, X = In, Sn) and analyzing the interaction between Cu or Ni *d*-electrons and In or Sn *s* and *p*-electrons. In this way, a microscopic interpretation was provided of their cohesive properties. Here we aim at presenting a more general discussion of the electronic properties of Me-X compounds (Me = Cu, Ni, X = In, Sn), and of how these properties evolve by increasing the amount of the non-transition metal element X in the compound. To this end, we will consider the specific cases of Ni–In and Cu–In ICs.

In Fig. 5 and 6, we plot the total DOS and site projected partial DOS (PDOS) for some selected Ni–In and Cu–In

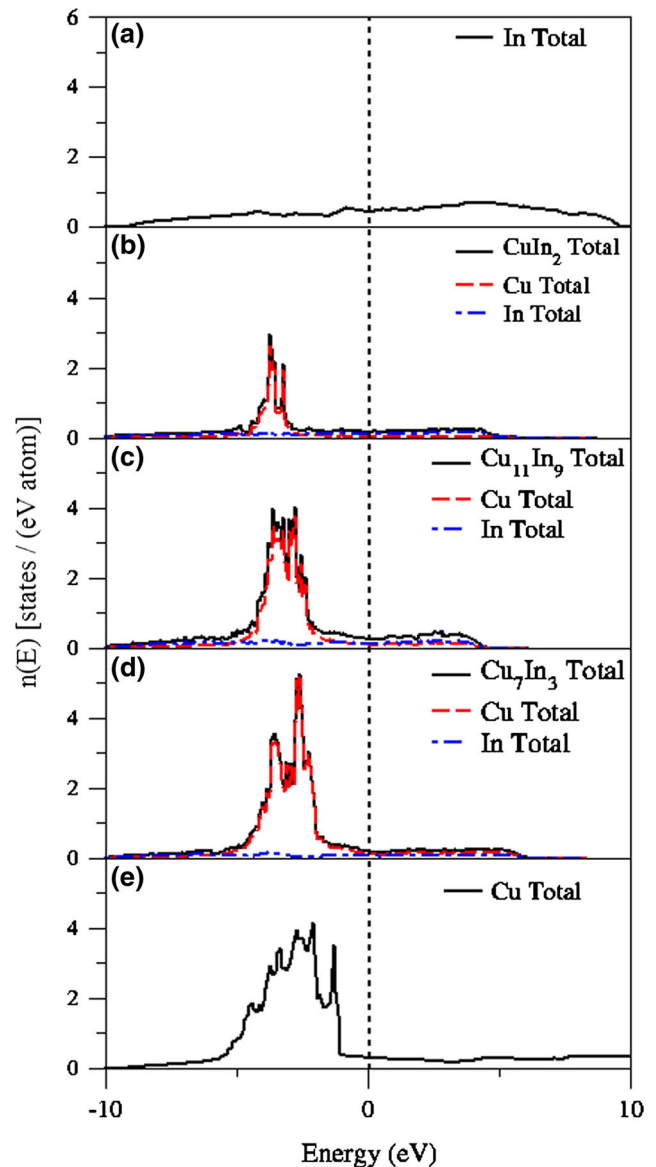


Fig. 6 Electronic density of states (DOS) for (a) In (tI2), (b) CuIn_2 (tI12), (c) $\text{Cu}_{11}\text{In}_9$ (mC20), (d) Cu_7In_3 (aP40), and (e) Cu (cF4). The atomic decomposed In (blue dash-dot lines) and Cu (red dashed lines) partial DOS are shown. The origin of the scale corresponds to the Fermi level (Color figure online)

stable compounds, at various compositions, including for comparison the DOS of their corresponding elements (Fig. 5a, e, 6a, e). The DOS of a compound is known to be essentially the result of the superposition of the bands of the constituting elements.^[28] In line with traditional models^[30] two main contributions to the electronic DOS can be identified for this family of compounds.^[10–13] There is a prominent peaked *d*-band arising from the atomic *d* transition element (Cu or Ni) orbitals, and superposed to this *d*-band, a broad *sp* free-electron-like band coming from the non-transition element (In in this case). As the amount of In is increased in the Ni–In and Cu–In compounds, the

number of Me–Me bonds (Ni–Ni or Cu–Cu) decreases and are replaced by Ni–In and Cu–In, respectively. The d band reduces its width and shifts to lower energies, leading to a decrease of the DOS at the Fermi level. This effect is more appreciable in the case of the Ni–In compounds.

By adding more In to the compounds, the Ni- d (for Ni–In ICs, Fig. 5) and Cu- d (for Cu–In ICs, Fig. 6) states are increasingly hybridized with the (mostly) p component of the free electron band. These p – d hybridization effects are thought to be the main binding effect stabilizing this type of compounds. The d -bands originated in Ni and Cu atoms are almost filled, and therefore bonding as well as anti-bonding states is occupied. Comparing the Ni–In and Cu–In cases, we note that their DOS are qualitatively similar, but the Cu- d band is shifted to lower energies compared with the corresponding Ni- d band. The expected anti-bonding states corresponding to the highest energy part of the DOS, are almost completely occupied in the Cu–In compounds, but partially and less occupied for the Ni compounds.

We remark that the general features of the DOS described above are common to all the compounds studied here despite their specific structures. The main difference between Cu–Sn and Ni–Sn compounds is that, since Sn has a higher number of valence electrons ($AGN = 4$), increased hybridization effects are expected, which explains the higher cohesion and more stability of the compounds for these systems.

The present trends in the electronic structure for the Ni–In compounds are also supported by classical experimental results of the electronic structure of the valence bands of Pd and Ni alloys obtained by x-ray photoelectron spectroscopy (XPS).^[31] In that work the authors report that in alloys with electropositive elements the Ni and Pd d -band centroids move to larger binding energies and the density of d states at the Fermi level is greatly decreased, indicating that the Ni and Pd d bands are being filled. The Ni and Pd d bands become narrower in alloys with more electropositive elements such as In and Al. The XPS results on NiIn (and various Ni–Al compounds) suggest an electronic structure behavior in line with the present theoretical findings for the Ni–In ICs.

6 Conclusions

The general aim of the present study is to use in depth a recently developed ab initio database to establish the systematics and interrelations between cohesive properties and EOS parameters for the Me_aX_b compounds formed by $Me = Cu, Ni$ and $X = In, Sn$. The current study indicates that the “ AGN ” is a useful variable in establishing trends appropriate to a further interpretation in terms of the electronic structure.

The work has also shown that the “ CED ” parameter, defined as E_{coh}/V_0 varies in a remarkably smooth fashion in Cu- X and Ni- X ($X = In, Sn$) compounds. Moreover, in agreement with previous results on the elemental solids^[22,39] it is shown that the E_{coh}/V_0 parameter can be related to the bulk modulus B_0 by a simple proportionality relation.

Furthermore, it has been shown that the ab initio energy versus volume results for the present compounds can be scaled in the way suggested by Rose, Ferrante and Smith for elemental solids. This fact is considered as a “higher degree of universality”. In addition, a “higher degree of universality” is found in the present work, which is used to explain the fact that for these compounds the E_{coh}/V_0 parameter is proportional to B_0 .

Finally, the paper also presents a microscopic interpretation of the variation of cohesive properties with this class of compounds in terms of the systematic changes in the contributions to the DOS, the hybridization between the d - and p -electrons and the progressive filling up of bonding and anti-bonding states. The picture of the bonding trends developed on these bases is shown to account for the trends in the present and previous theoretical as well as experimental results.

Acknowledgments This work was supported by Project PIP 112-20110100814 from CONICET and Project I197 from Universidad Nacional del Comahue.

References

1. M. Hillert, The Compound Energy Formalism, *J. Alloys Compd.*, 2001, **320**, p 161-176
2. R. Hiren, P.D. Howes, and S.E. Hamman, A Review: On the Development of Low Melting Temperature Pb-free Solders, *Microelectron. Reliab.*, 2014, **54**, p 1253-1273
3. J.L. Freer and J.W. Morris, Microstructure and Creep of Eutectic Indium/Tin on Copper and Nickel Substrates, *J. Electron. Mater.*, 1992, **21**(6), p 647-652
4. K.N. Tu and K. Zeng, Tin–Lead (SnPb) Solder Reaction in Flip Chip Technology, *Mater. Sci. Eng.*, 2001, **R34**, p 1-58
5. T.H. Chuang, C.L. Yu, S.Y. Chang, and S.S. Wang, Phase Identification and Growth Kinetics of the Intermetallic Compounds Formed During In–49Sn/Cu Soldering Reactions, *J. Electron. Mater.*, 2002, **31**(6), p 640-645
6. Dae-Gon Kim and Seung-Boo Jung, Interfacial Reactions and Growth Kinetics for Intermetallic Compound Layer Between In–48Sn Solder and Bare Cu Substrate, *J. Alloys Compd.*, 2005, **386**, p 151-156
7. S. Sommadossi and A. Fernández, Guillermet, Interface Reaction Systematics in the Cu/In–48Sn/Cu System Bonded by Diffusion Soldering, *Intermetallics*, 2007, **15**, p 912-917
8. C.-Y. Huang and S.-W. Chen, Interfacial Reactions in In–Sn/Ni Couples and Phase Equilibria of the In–Sn–Ni System, *J. Electron. Mater.*, 2002, **31**, p 152-160
9. S.-W. Chen, C.-H. Wang, and S.-K. Lin, Phase Diagrams of Pb-Free Solders and Their Related Materials Systems, *Lead-Free Electronic Solders, A Special Issue of the Journal of Materials*

- Science: Materials in Electronics*, K.N. Subramanian, Ed., Springer, Berlin, 2006, p 152-160
10. S. Ramos de Debiaggi, C. Deluque Toro, G.F. Cabeza, and A. Fernández Guillermet, Ab Initio Comparative Study of the Cu–In and Cu–Sn Intermetallic Phases in Cu–In–Sn Alloys, *J. Alloys Compd.*, 2012, **542**, p 280-292
 11. S. Ramos de Debiaggi, C. Deluque Toro, G.F. Cabeza, and A. Fernández Guillermet, Ab Initio Study of the Cohesive Properties, Electronic Structure and Thermodynamic Stability of the Ni–In and Ni–Sn Intermetallics, *J. Alloys Compd.*, 2013, **576**, p 302-316
 12. S. Ramos de Debiaggi, N.V. González Lemus, C. Deluque Toro, and A. Fernández Guillermet, Ab Initio Study of the Compound-Energy Modeling of Multisublattice Structures: The (hP6) Ni₂In-Type Intermetallics of the Ni–In–Sn System, *J. Alloys Compd.*, 2015, **619**, p 464-473
 13. S. Ramos de Debiaggi, N.V. González Lemus, G.F. Cabeza, and A. Fernández Guillermet, Cohesive Properties of (Cu, Ni)–(In, Sn) Intermetallics: Database, Electron–Density Correlations and Interpretation of Bonding Trends, *J. Phys. Chem. Solids*, 2016, **93**, p 40-51
 14. A. Fernández Guillermet and G. Grimvall, Cohesive Properties and Vibrational Entropy of 3d-Transition Metal Compounds: MX (NaCl) Compounds (X = C, N, O, S), Complex Carbides and Nitrides, *Phys. Rev. B*, 1989, **40**, p 10582-10593
 15. A. Fernández Guillermet and G. Grimvall, Bonding Properties and Vibrational Entropy of Transition Metal MeB₂ (AlB₂) Diborides, *J. Less Common Met.*, 1991, **169**, p 257-281
 16. J. Häglund, G. Grimvall, T. Jarlborg, and A. Fernández Guillermet, Band Structure and Cohesive Properties of 3d-Transition-Metal Carbides and Nitrides with the NaCl-Type Structure, *Phys. Rev. B*, 1991, **43**, p 14400-14408
 17. A. Fernández Guillermet and G. Grimvall, Cohesive Properties and Vibrational Entropy of 3d-Transition Metal Carbides, *J. Phys. Chem. Solids*, 1992, **53**, p 105-125
 18. A. Fernández Guillermet, J. Häglund, and G. Grimvall, Cohesive Properties of 4d-Transition Metal Carbides and Nitrides with the NaCl-Type Structure, *Phys. Rev. B*, 1992, **45**, p 11557-11567
 19. A. Fernández Guillermet, J. Häglund, and G. Grimvall, Cohesive Properties and Electronic Structure of 5d-Transition Metal Carbides and Nitrides with the NaCl-Type Structure, *Phys. Rev. B*, 1993, **48**, p 11673-11684
 20. J. Häglund, A. Fernández Guillermet, G. Grimvall, and M. Körling, Theory of Bonding in Transition Metal Carbides and Nitrides, *Phys. Rev. B*, 1993, **48**, p 11685-11691
 21. K.A. Gschneidner, Physical Properties and Interrelationships of Metallic and Semimetallic Elements, *Solid State Phys.*, 1964, **16**, p 275-426
 22. S. Wacke, T. Górecki, Cz Górecki, and K. Książek, Relations Between the Cohesive Energy, Atomic Volume, Bulk Modulus and Sound Velocity in Metals, *J. Phys. Conf. Ser.*, 2011, **289**(1), p 012020
 23. J.H. Rose, J.R. Smith, F. Guinea, and J. Ferrante, Universal Features of the Equation of State of Metals, *Phys. Rev. B*, 1984, **29**(6), p 2963-2969
 24. P. Vinet, J.R. Smith, J. Ferrante, and J.H. Rose, Temperature Effects on the Universal Equation of State of Solids, *Phys. Rev. B*, 1987, **35**(4), p 1945-1953
 25. C.D. Gelatt, A.R. Williams, and V.L. Moruzzi, Theory of Bonding of Transition Metals–Nontransition Metals, *Phys. Rev. B*, 1983, **27**(4), p 2005-2013
 26. R.E. Watson and L.H. Bennett, Optimized Prediction for Heats of Formation of Transition Metal Alloys, *Calphad*, 1981, **5**(1), p 25-40
 27. C. Colinet, A. Pasturel, and P. Hicter, Trends in Cohesive Energy of Transition Metal Alloys, *Calphad*, 1985, **9**(1), p 71-99
 28. C. Colinet and A. Pasturel, Trends in Cohesive Energy Transition Rare-Earth Metal Alloys, *Calphad*, 1987, **11**(4), p 335-348
 29. R.E. Watson, M. Weinert, J.W. Davenport, and G.W. Fernando, The Energetics of Transition Metal Alloy Formation: Theory Versus Experiment, *Scr. Metall.*, 1988, **22**, p 1285-1289
 30. J. Friedel, Transitions Metals, Electronic Structure of the d-Band. Its Role in the Crystalline and Magnetic Structures, *The Physics of Metals-1 Electrons*, J.M. Ziman, Ed., Cambridge University Press, Cambridge, 1969, p 340-403
 31. J.C. Fuggle, F.U. Hillebrecht, R. Zeller, Z. Zolnieriek, and P.A. Bennett, Electronic Structure of Ni and Pd Alloys. I. X-Ray Photoelectron Spectroscopy of the Valence Bands, *Phys. Rev. B*, 1982, **27**(4), p 2145-2178
 32. P.E. Blöchl, Projector Augmented-Wave Method, *Phys. Rev. B*, 1994, **B50**, p 17953-17979
 33. G. Kresse and J. Joubert, From Ultrasoft Pseudopotentials to the Projector Augmented-Wave Method, *Phys. Rev. B*, 1999, **B59**, p 1758-1775
 34. G. Kresse and J. Furthmüller, Efficiency of Ab-Initio Total Energy Calculations for Metals and Semiconductors Using a Plane-Wave Basis Set, *Comput. Mater. Sci.*, 1996, **6**, p 15-50
 35. J.P. Perdew and Y. Wang, Accurate and Simple Analytic Representation of the Electron–Gas Correlation Energy, *Phys. Rev. B*, 1992, **45**(23), p 13244-13249
 36. H.J. Monkhorst and J.D. Pack, Special Points for Brillouin-Zones Integrations, *Phys. Rev. B*, 1976, **13**, p 5188-5192
 37. M. Methfessel and A.T. Paxton, High-Precision Sampling for Brillouin-Zone Integration in Metals, *Phys. Rev. B*, 1986, **40**, p 3616-3621
 38. G. Ghosh, Elastic Properties, Hardness, and Indentation Fracture Toughness of Intermetallics Relevant to Electronic Packaging, *J. Mater. Res.*, 2004, **19**, p 1439-1454
 39. A.S. Mikhaylushkin, T. Sato, S. Carlson, S.I. Simak, and U. Häussermann, High-Pressure Structural Behavior of Large-Void CoSn-type Intermetallics: Experiments and First-Principles Calculations, *Phys. Rev. B*, 2008, **77**, p 014102(8)
 40. D.S. Bertoldi, S.B. Ramos, and A. Fernández Guillermet, Interrelations Between EOS Parameters and Cohesive Energy of Transition Metals: Thermostatistical Approach, Ab Initio Calculations and Analysis of “Universality” Features, *J. Phys. Chem. Sol.*, 2016 (**under review**)
 41. J.A. Garcés and A. Fernández Guillermet, Equation of State Parameters for Stable and Non-stable Transition Metal Phases from Universal Binding Energy Relation, *Calphad*, 1998, **22**, p 469-493